

PACS numbers: 42.65.Ky; 42.50.Hz
DOI: 10.1070/QE2001v031n02ABEH001913

High-order harmonic generation by multielectron atoms in the field of a relativistic-intensity standing electromagnetic wave

V D Taranukhin, N Yu Shubin

***Abstract*. A semiclassical model of high-order harmonic generation (HHG) is developed and applied for the investigation of HHG in relativistic-intensity laser fields. A shift of photoelectrons along the wave vector of the pump wave is shown to reduce the harmonic intensity. In the low-frequency range of the spectrum of high-order harmonics, this intensity lowering is more noticeable than in the high-frequency range. We propose to use a standing wave instead of a travelling wave to increase the HHG efficiency by reducing the longitudinal shift of photoelectrons. The efficiency of using atoms in a standing wave is shown to decrease with the growth in the pump intensity. However, in the case of a travelling wave, this decrease in the HHG efficiency is even more noticeable. The use of a standing wave provides a considerable increase in the HHG efficiency, which may be as high as $\sim 10^2$ when pump radiation has an intensity $I \approx 10^{18}$ W cm^{-2} and a wavelength of 0.3 μm.**

Keywords: *high-order harmonic generation, relativistic effects.*

1. Introduction

High-order harmonic generation (HHG) by atoms in strong laser fields (see, e.g., Refs [1, 2]) holds much promise for the generation of coherent X-ray radiation. The methods allowing the efficiency of this process to be increased and permitting the maximum possible radiation frequency to be achieved are of considerable interest. The spectrum of harmonics is usually characterised by a cut-off frequency $\Omega = N_{\max}\omega$ (where $N_{\max}$ is the maximum harmonic number and ω is the frequency of pump radiation). In the nonrelativistic limiting case, the cut-off frequency is determined by the following expression $\Omega_0 = U_p + 3.17U_q$ [1], where $U_q = F_0^2/4\omega^2$ is the ponderomotive energy; F_0 is the amplitude of the electric field strength in the pump wave; and U_p is the atomic ionisation potential (we employ the system of units where $e = m = \hbar = 1$). Thus, the pump intensity I should be increased to achieve the maximum radiation frequency.

However, the depletion of atomic states limits the maximum radiation frequency in HHG experiments performed with high pump intensities. The value of Ω_0 under these conditions is determined by the ionisation saturation intensity I_s for a given atom rather than by the peak intensity in the pump pulse. On the other hand, harmonics produced by singly and doubly charged ions have been also observed in experiments [2]. The values of Ω_0 in these experiments exceeded the values of this parameter typical of neutral atoms since ions possess higher energies U_p and, consequently, have higher energies U_q for the saturation intensity I_s. Thus, harmonics with higher orders can be produced when ions with a higher charge are irradiated by pump pulses with intensity I considerably exceeding the saturation intensity I_s for neutral atoms.

High pump intensities (e.g., $I \approx 10^{17}$ W cm^{-2} is achieved at the wavelength $\lambda = 0.3$ μm in experiments [2]) should give rise to relativistic effects in HHG [3 – 6]. Note that the bremsstrahlung emission of a photoelectron perturbed by the field of a parent ion has been calculated in Ref. [3]. Generation of high-order harmonics under these conditions is due to the recombination of photoelectrons with a parent ion [4 – 6]. The interaction of photoelectrons with the magnetic component of pump radiation, which shifts photoelectrons along the wave vector of the travelling pump wave, plays an important role in both cases. Because of this shift, a photoelectron returning to its parent ion misses this ion, and the HHG efficiency lowers. In our papers [6], we proposed to employ a standing wave to solve this problem.

In this study, relativistic effects in HHG in the field of both travelling and standing waves are analysed within the framework of a semiclassical model. Quantum-mechanical calculations of HHG spectra will be also presented.

2. The quantum-mechanical model of high-order harmonic generation in relativistic-intensity fields

In Refs [5 – 7], we have developed an approach to the description of HHG in the case when an isolated atom interacts with high-power laser radiation. This approach follows the general scheme developed in Ref. [8]. However, the authors of Ref. [8] consider only the case of a low ionisation probability, ignoring the Coulomb interaction of photoelectrons with a parent ion as well as relativistic effects accompanying the motion of a photoelectron in the continuum. In this paper, we propose an illustrative quantum-mechanical model, which includes all these effects, thus allowing HHG in relativistic-intensity pump fields to be investigated.

The expression for the field-induced dipole moment responsible for HHG derived in Ref. [5] can be interpreted

V D Taranukhin, N Yu Shubin International Teaching and Research Laser Centre, M V Lomonosov Moscow State University, Vorob'evy gory, 119899 Moscow, Russia

Received 29 September 2000
Kvantovaya Elektronika **31** (2) 179 – 184 (2001)
Translated by A M Zheltikov

in a physically instructive way. A photoelectron wave packet is produced in the continuum at the first stage of the considered process. The amplitude of this wave packet is determined by the probability W of tunnelling ionisation [9]. At the next stage, the wave packet, which was assumed to have a Gaussian shape in our calculations, evolves in the pump field, with its width σ growing with a rate

$$V_{\rm sp} \approx F^{1/2}(2U_{\rm p})^{-1/4} \tag{1}$$

(see [10]), which agrees well with the experimental data [11]. The trajectory of the centre of the packet is governed by the classical equation of motion, which relates the coordinate r of the centre of the wave packet to its velocity v. Taking into consideration also the Coulomb electron-ion interaction, we arrive at

$$\frac{{\rm d}v}{{\rm d}t} = \left(1 - \frac{v^2}{c^2}\right)^{1/2}\left\{-\boldsymbol{F} - \frac{1}{c}[\boldsymbol{v}\boldsymbol{B}] - Z\frac{\boldsymbol{r}}{r^3} + \frac{1}{c^2}\boldsymbol{v}\left[\boldsymbol{v}\left(Z\frac{\boldsymbol{r}}{r^3} + \boldsymbol{F}\right)\right]\right\}, \tag{2}$$

$$r(t_0) = r_0, \quad v(t_0) = v_0,$$

where $\boldsymbol{B}$ is the induction of the magnetic field in pump radiation, Z is the charge of the ion residual, and r_0 and v_0 are the initial coordinate and the velocity of the electron, respectively. In the case of a two-component pump field, we have $F = F_1(\zeta_1)\cos\zeta_1 + F_2(\zeta_2)\cos\zeta_2$, $B = B_1(\zeta_1)\cos\zeta_1 + B_2(\xi_2)\cos\zeta_2$, and $\zeta_{1,2} = \omega_{1,2}t - k_{1,2}r$, where $\omega_{1,2}$ and $k_{1,2}$ are the frequencies and wave vectors, respectively; and $F_{1,2}$ and $B_{1,2}$ are the amplitudes of the electric and magnetic components of the pump field, respectively. In the regime of tunnelling ionisation, an electron starts its motion in the continuum from the outer boundary of the potential barrier at the moment of time t_0, and we can set $v_0 \approx 0$ [1].

When this electron returns to its parent ion, it may recombine, emitting a quantum with an energy $N\omega$. The intensity I_N of recombination emission at the frequency $N\omega$ (where N is the harmonic number) is proportional to the modulus squared of the Fourier transform of the second-order time derivative taken for the matrix element of the dipole moment.

The case of incommensurate frequencies ω_1 and ω_2 was considered in our papers [7, 12]. The case when $\omega_1 = \omega_2$ corresponds to a monochromatic pump field. Provided that $F_1 = F_2$, $B_1 = B_2$, and $k_1 = -k_2$, the pump has a form of a standing wave. Thus, the approach described above includes the three-dimensional character of electron motion in the continuum and relativistic effects. This approach can be employed to consider laser fields of an arbitrary configuration.

3. A semiclassical analysis of high-order harmonic generation

3.1 A travelling wave

A semiclassical analysis of HHG can be performed on the basis of Eqns (1) and (2). According to the model [1], high-order harmonics are mainly generated by photoelectrons that return to a parent ion and recombine, emitting a quantum whose frequency is determined by the kinetic energy $E_{\rm r}$ of electrons at the moment $t_{\rm r}$ of recombination. Thus, the cut-off frequency Ω is determined by the maximum energy $E_{\rm r}^{\rm max}$ of a photoelectron returning to its parent ion and the ionisation potential of an atom (ion). Note that an important feature distinguishing the proposed semiclassical model from the model developed in Ref. [1] is the inclusion of the magnetic component of pump radiation and the spreading of the photoelectron wave packet. In addition, we also take into account the dependence of the packet spreading rate on the electric field strength F and on the atomic ionisation potential $U_{\rm p}$.

Consider the interaction of an electron with a linearly polarised plane electromagnetic wave (F_x, B_y) propagating along the z-axis. In this case, the electron energy $E_{\rm r}$ is highly sensitive to the ionisation moment t_0 and is described by a nonmonotonic function of this moment [1, 4] (Fig. 1). Let us introduce an optimal ionisation moment $t_{\rm opt}$ corresponding to $E_{\rm r} = E_{\rm r}^{\rm max}$. Since electrons returning to their parent ions provide a dominant contribution to HHG, we restrict our analysis to the values of t_0 falling within the range of 1/4 of the pump cycle T ($0 < t_0 < T/4$). In the nonrelativistic case, we have $\omega t_{\rm opt} \approx \pi/10$ [4] and $\Omega = \Omega_0 = U_{\rm p} + 3.17U_{\rm q}$. In the relativistic regime, the maximum frequency Ω may be less than Ω_0.

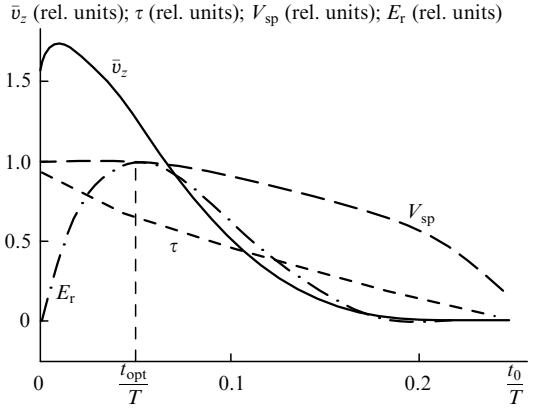

Figure 1. The time of motion in the continuum, $\tau = t_{\rm r} - t_0$, calculated with Eqn (4); the mean velocity of longitudinal motion $\bar{v}_z = z_{\rm r}/\tau$ in a travelling wave; the rate of spreading of the photoelectron wave packet, $V_{\rm sp}$; and the kinetic energy of a photoelectron, $E_{\rm r}$, as functions of the moment t_0 of ionisation of the electron. Calculations were performed within the framework of the semiclassical model including relativistic effects in the first-order approximation in v/c for a travelling pump wave.

Note that for relatively low pump intensities I, electrons move along the direction of polarisation of the electric field. The longitudinal shift z accompanying the increase in I reduces the recombination probability and, consequently, lowers the intensities of high-order harmonics. This longitudinal shift depends on both pump parameters (I and ω) and t_0. Note that the dependence of z on t_0 changes the shape of the HHG spectrum since electrons emerging into the continuum at different moments t_0 contribute to different regions of this spectrum.

For moderate pump intensities, Eqn (2) can be solved by the method of successive iterations with a small parameter v/c. In the zeroth-order approximation in v/c, an electron is involved in a one-dimensional motion along the x axis:

$$x(t) = x_0[\cos\omega t - \cos\omega t_0 + \omega(t - t_0)\sin\omega t_0],$$
$$v_x(t) = \omega x_0(\sin\omega t_0 - \sin\omega t), \tag{3}$$

where $x_0 = F_0/\omega^2$. Let us introduce the time $\tau \equiv t_r - t_0$ of photoelectron motion in the continuum. Taking into account that a photoelectron returns to its parent ion, i.e., $x(t_r) = 0$, we can apply Eqn (3) to find an implicit expression for the dependence $\tau(t_0)$):

$$t_0 = \frac{1}{\omega}\arctan\frac{1-\cos\omega\tau}{\omega\tau-\sin\omega\tau}, \tag{4}$$

This dependence is described by a monotonically decreasing function (see Fig. 1).

In the next-order approximation in v/c, a photoelectron acquires an additional motion along the z-axis: $z(t) = z_0 f(t_0,t_r)$, where

$$z_0 = \frac{F_0^2}{c\omega^3};$$

$$f(t_0,t) = -\frac{\sin 2\omega t}{8} + \sin\omega t_0(\cos\omega t - \cos\omega t_0) + \omega(t-t_0)$$
$$\times\left(\sin^2\omega t + \frac{\cos 2\omega t_0}{4}\right) + \frac{\sin 2\omega t_0}{8}; \tag{5}$$
$$v_z = \omega z_0\left(-\frac{\cos 2\omega t}{4} - \sin\omega t_0\sin\omega t + \frac{1}{4} + \frac{\sin^2\omega t_0}{2}\right).$$

One can see from these expressions that an electron is now involved in drift and oscillatory motion along the z-axis at the fundamental and doubled frequencies with a velocity $v_z \sim I/(c\omega^2)$. Thus, the longitudinal shift of a photoelectron is a quantity of the first order in v_x/c. Consequently, this effect should manifest itself even at relatively low radiation intensities (numerical estimates are presented below in this section).

Consider the influence of the longitudinal shift z of a photoelectron on HHG taking into account the dependences of z on I, ω, and t_0 obtained by successive iterations. Let us introduce the notations $z_r(t_0) = z(t_0, t_r)$, and $f_r(t_0) = f(t_0, t_r)$. Using numerical methods to solve Eqn (4) and substituting the results into Eqn (5), we can determine the dependence $z_r(t_0)$ of the longitudinal shift of a photoelectron at the moment when it returns to its parent ion. This dependence is described by a monotonically decreasing function, which is confirmed by the results of direct numerical simulations using Eqn (2). The mean velocity $\bar{v}_z \equiv z_r(t_0)/\tau(t_0)$ of longitudinal motion in a travelling wave decreases for all the values of t_0, except for a narrow range of small t_0, where $\bar{v}_z$ slightly increases (see Fig. 1).

Let us introduce a criterion that an electron wave packet with a width $V_{sp}\tau$ misses its parent ion:

$$z_r(t_0) > V_{sp}\tau(t_0). \tag{6}$$

We assume that, when condition (6) is satisfied, a photoelectron does not contribute to recombination emission, which decreases the intensity of the relevant harmonics. The dependences of the energy E_r and the shift z_r on t_0 change the shape of the harmonic spectrum. With $t_0 \approx 0$, the electron energy $E_r(t_0)$ is low (Fig. 1), while the ionisation probability and the shift z_r are large. Therefore, we should expect a noticeable decrease in the intensity of harmonics in the low-frequency region of the spectrum (as compared with the nonrelativistic case).

When the pump intensity becomes higher than some characteristic intensity I_t, criterion (6) is satisfied for electrons with $t_0 \geqslant t_{opt}$. Under these conditions, E_r^{max} becomes less than $3.17U_q$ (Fig. 2). With a further increase in I, the growth rate of E_r^{max} and, consequently, the growth rate of the maximum radiation frequency Ω decrease (Fig. 2). The parameter E_r^{max} decreases due to the fact that only electrons with lower energies can efficiently recombine, returning to the vicinity their parent ions, while electrons with $t_0 \approx t_{opt}$ miss their parent ions, giving no contribution to HHG.

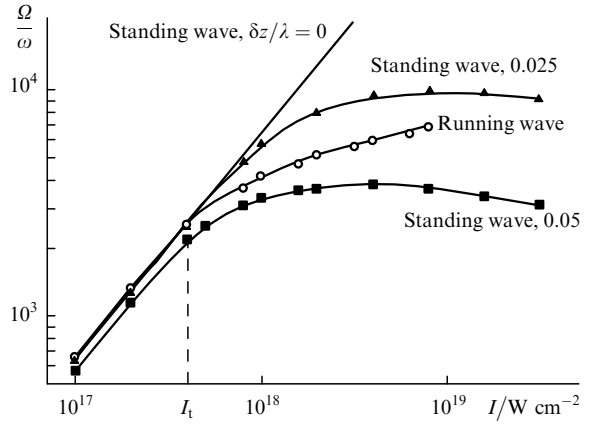

Figure 2. Dependences of the maximum harmonic frequency Ω on the intensity I of pump radiation with a wavelength $\lambda = 308$ nm in the travelling- and standing-wave regimes for different $\delta z/\lambda$. Calculations were performed within the framework of the semiclassical model for an Ar^{8+} ion (the ionisation potential is $I_p = 15.5$ a.u.).

Let us estimate the critical intensity I_t. Using Eqn (6) and invoking an estimate for the mean velocity of longitudinal motion $\bar{v}_z$, we find that $\bar{v}_z > V_{sp}$. Then, Eqns (1) and (5) yield $I_t = c^{4/3}\omega^{8/3}(2I_p)^{1/3}[\omega\tau/f_r(t_0)]^{2/3}$, and the relevant cut-off frequency is $\Omega_{cr} \sim \omega^{2/3}$. Thus, the criterion of relativistic regime in HHG can be written as $I(\lambda/2\pi)^{8/3} > c^4$ (i.e., $I_t \sim \lambda^{-8/3}$). This condition considerably differs from the generally accepted criterion of relativistic regime in above-threshold ionisation, formulated in terms of the increase in the effective electron mass $(I(\lambda/2\pi)^2 > c^4$, which corresponds to $I > 10^{18}$ W cm^{-2} for $\lambda = 1$ μm [3]). Consequently, the influence of the magnetic component of the pump field on HHG should be taken into account for radiation with $\lambda = 0.3$ μm already starting with $I = 10^{17}$ W cm^{-2}.

3.2 A standing wave

To prevent the decrease in the HHG efficiency due to the longitudinal shift of photoelectrons, we propose to use a standing wave for pumping. In such a wave, the amplitude of pump components acting on an atom depends on the position δz of atoms. Electric-field antinodes ($\delta z = 0$) correspond to the nodes of the magnetic field. Consequently, the magnetic-field force acting on an electron is equal to zero at these points. The amplitude of the electric field decreases as $\sim\cos(2\pi\delta z/\lambda)$, while the amplitude of the magnetic field increases as $\sim\sin(2\pi\delta z/\lambda)$ away from these points. This implies that the longitudinal drift can be offset and, consequently, the HHG efficiency can be improved only within some part of the interaction volume. Furthermore, the decrease in the amplitude of the electric field reduces the ponderomotive energy of an electron. Therefore, when high-order harmonics are generated by atoms located at points with different δz, quanta with a fixed energy are emitted by photoelectrons with different t_0. This feature distinguishes the case of a standing wave from the

regime of a travelling wave, where such a dependence may be only due to a transverse intensity distribution in a confined pump beam.

In the case of a standing wave, criterion (6), which determines the HHG efficiency, remains the same as in the regime of a travelling wave. The spreading of the electron wave packet occurs in a similar way in these two cases. The scenario of this spreading is equivalent to the spreading of a free wave packet. The latter circumstance is one of the assumptions of the employed model, which relies on the fact that a considerable part of the photoelectron trajectory in the continuum lies far from the parent ion and the Coulomb field only slightly influences this spreading. Thus, the analysis of relativistic effects in HHG in a standing wave is reduced to the investigation of the longitudinal shift of a photoelectron.

In the first-order approximation in v/c, the electron motion in a standing wave along the x-axis is the same as in the nonrelativistic regime. The differences from the case of a travelling wave [i.e., from Eqns (3)] are noticeable under these conditions only in the dependence of the amplitudes of the photoelectron coordinate and velocity on the position of an atom δz. The equation governing the photoelectron motion along the z-axis in a standing wave is reduced to a nonlinear Hill equation. An analytical investigation of this equation encounters considerable difficulties. However, for relatively low intensities, when $(z-\delta z)/\lambda \sim U_q/c^2 \ll 1$, we can assume that the amplitude of the field acting on an electron is independent of the current coordinate of the electron (depending only on the coordinate of the atom). In such a situation, we have $\sin(4\pi z/\lambda) \approx \text{const} = \sin(4\pi\delta z/\lambda)$. This approximation remains valid also for small δz, i.e., for atoms located around antinodes of the electric field, since the amplitude of the longitudinal shift of electrons decreases accordingly.

This approximation gives the following expression for the longitudinal shift of a photoelectron:

$$z = z_0 g(t_0, t)\sin(4\pi\delta z/\lambda)/2 + \delta z,$$

where

$$\begin{aligned} g(t_0,t) &= \{1/2 + \omega(t-t_0)[\omega(t-t_0) - \sin 2\omega t_0]/4 \\ &\quad - \sin\omega t_0 \sin\omega t + (\cos 2\omega t_0 - 5\cos 2\omega t)/8\}; \\ v_z &= \omega z_0 \sin(4\pi\delta z/\lambda)/2[\omega(t-t_0) - (\sin 2\omega t + \sin 2\omega t)/4 \\ &\quad - \sin\omega t_0 \cos\omega t]. \end{aligned} \tag{7}$$

Numerical integration of Eqn (2) for a standing wave with $\lambda = 0.3$ μm and the values of I up to 10^{19} W cm^{-2} shows that, even with very small $\delta z/\lambda \sim 0.01$, Eqn (7) is satisfied with an error not exceeding 10 %. As can be seen from Eqn (7), in contrast to the case of a travelling wave described by Eqn (5), the motion of a photoelectron in a standing wave has an additional (uniformly accelerated) component. At the moments of recombination, this component dominates over the oscillatory and drift components for ionisation moments $t_0 \approx t_{\text{opt}}$ [the shift $z_r(t_{\text{opt}})$ due to this component exceeds the shift related to all the other components by an order of magnitude].

Applying Eqns (5) and (7) to compare the electron shifts $z_r(t_0)$ in travelling and standing waves, we find that, in the case when the pump intensity remains the same and the inequality

$$\sin|4\pi\delta z/\lambda| < \frac{f_r(t_0)}{g_r(t_0)}, \tag{8}$$

is satisfied, where $g_r(t_0) = g(t_0, t_r)$, the shift $z_r(t_0)$ in a travelling wave exceeds the corresponding shift in a standing wave. Inequality (8) allows us to estimate the range of values of $\delta z < \delta z_{cr}$ where the HHG efficiency in a standing wave is higher than the HHG efficiency in a travelling wave (for the same pump intensity). Note that this estimate is independent of atomic parameters and the pump intensity, depending only on the ionisation moment. Solving numerically Eqns (4) and (8) for δz_{cr}, we obtain $\delta z_{cr}(t_{\text{opt}})/(\lambda/4) \approx 0.12$. Consequently, not all the atoms provide equivalent contributions to HHG in a standing wave. The parameter $\delta z_{cr}/(\lambda/4)$ under these conditions characterises the efficiency of utilising atoms in this process.

In the case of a Gaussian wave packet [11], condition (6) does not necessarily imply that an electron misses its parent ion. It rather implies a decrease in the recombination probability and, consequently, the lowering of the HHG efficiency. With relativistic pump intensities, frequency components close to Ω_0, but possessing much lower intensities should be expected in HHG spectra under these conditions for both travelling- and standing-wave regimes. Note also that the width of the wave packet $\sigma(t_r)$ usually substantially exceeds the width of the wave function of the atomic ground state. The intensity I_N of the Nth harmonic in this case is determined by the shape of the electron wave packet and is characterised by a Gaussian dependence on the longitudinal shift of the centre of the wave packet:

$$I_N \sim \exp\left[-2\left(\frac{z_r(t_0)}{V_{sp}\tau(t_0)}\right)^2\right]. \tag{9}$$

The factor (9) determines the relativistic modification of the HHG spectrum and allows the estimation of the decrease η_t in harmonic intensities in a travelling wave relative to the standing-wave regime for $\delta z = 0$. Invoking Eqns (1), (5), and (7), we arrive at

$$\eta_t(t_0) \approx \exp\left(-2a_f^2(t_0)\right), \tag{10}$$

where $a_f(t_0) = F^{3/2}(2I_p)^{1/4} f_r(t_0)/(\omega^3 c\tau(t_0))$. Fig. 3 presents the dependence of $\eta_t(t_{\text{opt}})$ on the pump intensity. This dependence shows that, as the pump intensity I grows from I_t up to $2I_t$, the harmonic intensity lowers by two orders of magnitude, and the efficiency of using a travelling wave becomes very low for $I > I_t$. Expression (9) also gives the following estimate for the decrease in the intensity of harmonics generated by atoms with $\delta z \neq 0$ in the standing-wave regime relative to the intensity of harmonics generated by atoms with $\delta z = 0$:

$$\eta_s(t_0, \delta z) \approx \exp\left(-a_g^2(t_0)\sin^2\frac{4\pi\delta z}{\lambda}\right), \tag{11}$$

where $a_g(t_0) = F^{3/2}(2I_p)^{1/4} g_r(t_0)/(\omega^3 c\tau(t_0))$.

Note that, due to the nonmonotonic character of the dependence $E_r(t_0)$, two classical trajectories contribute to radiation emission at frequencies lower than Ω_0. Specifically, for the frequency equal to $\Omega_0/2$, we have to take into consideration ionisation moments $t_0 \approx t_1 = 0.01T$ and $t_2 = 0.1T$ (see Fig. 1). The ionisation probability calculated for t_1 in the case of Ar^{8+} ions in the presence of a pump field with $I \sim 10^{18}$ W cm^{-2} is eight orders of magnitude higher than the ionisation probability for t_2. Therefore, the left-hand branch ($0 < t_0 < t_{\text{opt}}$) of the curve representing E_r in

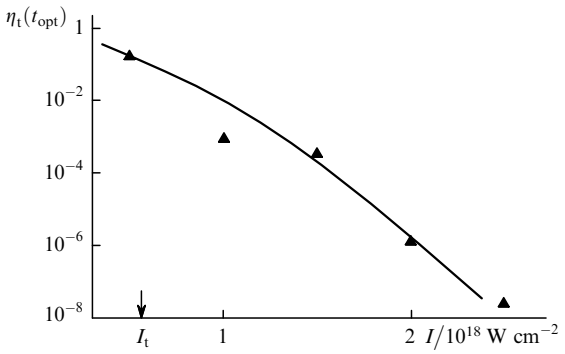

Figure 3. Results of (curve) semiclassical and (dots) model quantum-mechanical calculations for the ratio $\eta_t(t_{opt})$ of the intensities of the harmonic with the frequency equal to $3.17U_q$ in travelling and standing waves (for $\delta z = 0$) as a function of the pump intensity.

Fig. 1 provides a dominant contribution to HHG. The parameter $\alpha = (\bar{v}_z(t_0)/\bar{v}_z(t_{opt}))^2$ for t_1 is equal to 1.8 for a travelling wave and 1.4 for a standing wave. As can be seen from Eqns (10) and (11), parameters characterising the decrease in the harmonic intensity in the central part of the plateau and around its cut-off are related to each other in the following way:

$$\eta_{s,t}(t_1) \sim \eta^{\alpha}_{s,t}(t_{opt}). \tag{12}$$

Since $\alpha > 1$, the decrease in the harmonic intensity in the central part of the plateau is more noticeable than a similar decrease around the plateau cut-off (a dip in the plateau). This effect is due to a decrease in the mean velocity $\bar{v}_z$ of longitudinal motion and the growth in the photoelectron energy E_r with an increase in t_0 for $t_0 < t_{opt}$ (Fig. 1). Thus, the developed model predicts a relativistic lowering in the intensities of all the harmonics and a noticeable dip in the plateau within the low-frequency region of the HHG spectrum.

Let us estimate the total efficiency ξ of Nth-harmonic generation by atoms with different δz in a standing wave. For this purpose, we integrate the dependence $\eta_s(\delta z)$, which yields

$$\xi = \frac{4}{\lambda}\int_0^l \mathrm{d}z \exp\left[-\frac{1}{2}a_g^2(t_0)\sin^2(2k\delta z)\right], \tag{13}$$

where $l = \lambda/2\pi \arccos(N\omega/\Omega_0)$ determines the maximum value of δz that still allows the generation of the Nth harmonic (since $N\omega < \Omega = \Omega_0 \cos^2 k\delta z$). Note that ξ can be quite arbitrarily called the efficiency of utilising atoms in a standing wave. Generation of high-order harmonics with maximum frequencies is of particular interest. Therefore, the value of l is small in the estimate of Eqn (13) for N close to Ω_0/ω, and we can assume that $\sin(2k\delta z) \approx 2k\delta z$. If we neglect a weak dependence of t_0 on δz (for $0 < \delta z < l$), integration in Eqn (13) yields

$$\xi = \left(\frac{2}{\pi}\right)^{1/2} \frac{\mathrm{erf}(2^{1/2}\pi l a_g/\lambda)}{a_g}, \tag{14}$$

where $\mathrm{erf}\, x$ is the error function. Thus, the total HHG efficiency in the standing-wave regime decreases with the growth in I, as can be seen from Eqns (10), (11), and (14), but much slower than in the travelling-wave regime. Estimates performed for $N\omega = 0.9\Omega_0$, $I = 10^{18}$ W cm^{-2}, and $\lambda = 0.3\mu$m demonstrate that $\xi \approx 7 \times 10^{-2}$ and $\eta_t \approx 7 \times 10^{-4}$. Therefore, the enhancement R of the HHG efficiency in the standing-wave regime relative to the travelling-wave regime is $\xi/\eta_t \approx 10^2$. Note that this enhancement should be even higher for the central region of the plateau.

Thus, semiclassical calculations provide a clear understanding of the influence of relativistic effects on HHG. To confirm the predictions of our semiclassical approach for HHG in the relativistic regime, we carried out quantum-mechanical calculations for the spectra of short-wavelength emission of atoms.

3.3 Calculation of HHG spectra within the framework of the quantum-mechanical model

Spectra of HHG were calculated for Ar^{8+} ions in the field of pump radiation with $\lambda = 0.3$ μm and $I \sim 10^{16}$–10^{19} W cm^{-2}. The trajectories of the centre of the wave packet were determined by the numerical integration of Eqn (2). The time dependences of electron coordinates were then substituted into the expression for the dipole moment $D(t)$ of the relevant free–bound transition, The current width of the wave packet was included through Eqn (1). The HHG spectrum was calculated by the method of stationary phase.

Consider first the relativistic modification of the HHG spectrum in the travelling-wave regime. The increase in the pump intensity ($I > I_t$) first results in a substantial lowering in the intensity of the low-frequency part of the HHG spectrum (Fig. 4). This result is consistent with Eqn (12) derived within the framework of the semiclassical model. A dip in the plateau appears due to the fact that a photoelectron misses its parent ion. Electrons with smaller t_0 are characterised by larger impact parameters, which corresponds to the low-frequency region of the spectrum. Such an interpretation is confirmed by the results of the following numerical simulation. Curve *3* in Fig. 4 represents the results of simulations performed for HHG in a standing wave for $\delta z = 0$ where the contribution of electrons with $t_0 < t_{opt}$ was artificially excluded (which is equivalent to a situation when such electrons miss their parent ions). The low-frequency part of the spectrum in this case coincides with the low-frequency spectral region in the travelling-wave regime. This coincidence confirms our interpretation of the dip in the plateau, since for high pump intensities, electrons with $t_0 < t_{opt}$ miss their parent ions in a travelling wave and provide a dominant contribution to HHG in a standing wave, thus ensuring the advantage of the standing-wave regime.

With a further increase in the intensity of a travelling wave, the intensity of the high-frequency part of the HHG spectrum also lowers (relative to the HHG spectrum in a standing wave for $\delta z = 0$). The intensity of the harmonic with the frequency $\Omega_0 = 3.17U_q$ is lower under these conditions than the intensity of the same harmonic produced in a standing wave for $\delta z = 0$. The dots in Fig. 3 show the ratio $\eta_t(t_{opt})$ of the intensities of this harmonic calculated for travelling and standing waves. This plot demonstrates a good agreement between the results of semiclassical analysis and model calculations of the spectrum. Thus, the ratio of the intensity of the harmonic with the frequency Ω_0 in a travelling wave to the intensity of this harmonic in a standing wave for $\delta z = 0$ may be as low as 5×10^{-4} for $I = 10^{18}$ W cm^{-2} (Figs 3, 5).

In the case of a standing-wave pump, the harmonic intensity also depends on the position of atoms: the harmonic

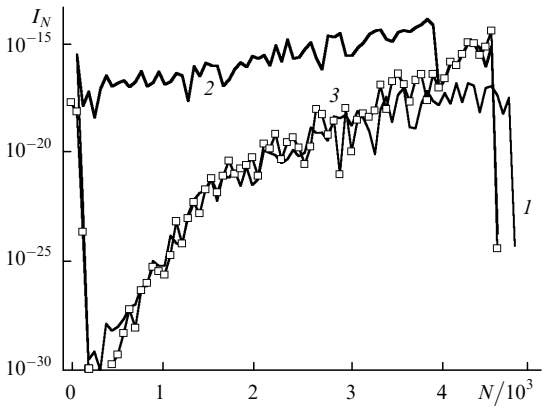

Figure 4. Results of quantum-mechanical calculations for HHG spectra of Ar^{8+} ions in a pump field with $I = 8 \times 10^{17}$ W cm^{-2} in (*1*) the travelling-wave regime and (*2*, *3*) the standing-wave regime for (*2*) $\delta z = 0$ and (*3*) $\delta z = 0$ when only the contribution of electrons with $t_0 > t_{opt}$ is included.

intensity decreases with the increase in δz. Furthermore, the quiver energy U_q and, consequently, Ω_0 lower because of the decrease in the amplitude of the electric field. Fig. 5 displays a series of HHG spectra in a standing wave for different δz. For comparison, this figure also presents the HHG spectrum in the travelling-wave regime for the same pump intensity. As can be seen from the comparison of these plots, the harmonic intensity in a standing wave for sufficiently small δz is higher than the harmonic intensity in a travelling wave, while for large δz, the harmonic intensity in a standing wave is lower than the harmonic intensity in a travelling wave. Thus, we can find the range $0 < \delta z < \delta z_{cr}$ where HHG in a standing wave is more efficient than HHG in a travelling wave. For the cut-off frequency, we have $\delta z_{cr}/(\lambda/4) \approx 0.1$, which is consistent with predictions of the semiclassical model.

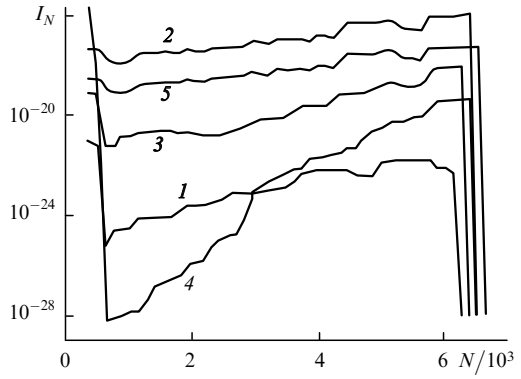

Figure 5. Results of quantum-mechanical calculations for HHG spectra of Ar^{8+} ions in a pump field with $I = 10^{18}$ W cm^{-2} and $\lambda = 308$ nm in (*1*) the travelling-wave regime and (*2*–*4*) the standing-wave regime for (*2*) $\delta z/\lambda = 0$, (*3*) 0.0125, and (*4*) 0.025. Curve *5* represents the total spectrum of harmonics emitted by a single atom within the range $0 < \delta z < \lambda/4$ in the standing-wave regime.

The response of the medium (per single atom) calculated by summing the HHG spectra generated by atoms with different δz in a standing wave is shown by curve *5* in Fig. 5. One can see that the harmonic intensity in the total spectrum is lower than the harmonic intensity in the optimal regime for $\delta z = 0$. This is due to the fact that the efficiency of utilising atoms $\xi < 1$ is less than unity [see the estimates performed with the use of Eqn (14)]. Thus, the enhancement R in HHG efficiency in the standing-wave regime relative to the travelling-wave regime is determined by two factors: the increase in the harmonic intensity for an atom at the point $\delta z = 0$ (with respect to the travelling-wave regime), which is characterised by the parameter $1/\eta_t$, and the efficiency ξ of utilising atoms in a standing wave. The enhancement R increases with the growth in the pump intensity and may reach several orders of magnitude. In particular, with $I = 10^{18}$ W cm^{-2} and $\lambda = 0.3$ μm, we have $\eta_t \approx 5 \times 10^{-4}$, $\xi \approx 5 \times 10^{-2}$, and $R \approx 10^2$.

4. Conclusions

Thus, the developed model predicts a considerable lowering in the intensity of high-order harmonics and modification of the shape of the harmonic spectrum in the case when relativistic-intensity pump radiation is used. The proposed scheme of HHG in a standing wave allows this lowering in the efficiency of harmonic generation to be partially compensated. In contrast to the case of a travelling-wave pump, the efficiency of harmonic generation in a standing wave is highly sensitive to the position of the atom emitting harmonics relative to an antinode of the electric field. Because of this factor, the efficiency ξ of utilising atoms in a standing wave is lower than the efficiency of utilising atoms in a travelling wave. This efficiency lowers with the growth in the pump intensity. However, due to the compensation of the relativistic shift of photoelectrons, the harmonic intensity in a standing wave may considerably exceed the intensity of harmonics in a travelling wave. In particular, the enhancement of HHG efficiency due to the use of a standing wave may be as high as 10^2 for a pump with an intensity of 10^{18} W cm^{-2} and a wavelength of 0.3 μm. This enhancement in the HHG efficiency increases with a further growth in the pump intensity.

Acknowledgements. This study was partially supported by the Russian Foundation for Basic Research, Grant No. 00-02-17533.

References

1. Corkum P B *Phys. Rev. Lett.* **71** 1994 (1993)
2. Preston S G, Sanpera A, Zepf M, et al. *Phys. Rev. A* **53** R31 (1996)
3. Keitel C H, Knight P L *Phys. Rev. A* **51** 1420 (1995)
4. Kulyagin R V, Shubin N Yu, Taranukhin V D *Proc. SPIE* **2770** 46 (1995)
5. Kulyagin R V, Taranukhin V D *Laser Phys.* **7** 623 (1997)
6. Taranukhin V D, Shubin N Yu *Book of Abstracts VIII Annual Intern. Laser Physics Workshop* (Budapest, Hungary, 1999), p. 103; Taranukhin V D *Laser Phys.* **10**, 330 (2000)
7. Taranukhin V D, Shubin N Yu *Kvantovaya Elektron.* **28** 81 (1999) [*Quantum Electron.* **29** 638 (1999)]
8. Lewenstein M, Balcou Ph, Ivanov M Yu, et al. *Phys. Rev. A* **49** 2117 (1994)
9. Keldysh L V *Zh. Eksp. Teor. Fiz.* **47** 1945 (1964)
10. Perelomov A M, Popov V S, Terent'ev M V *Zh. Eksp. Teor. Fiz.* **51** 309 (1966)
11. Budil K S, Salieres P, L'Huillier A, et al. *Phys. Rev. A* **48** R3437 (1993)
12. Taranukhin V D, Shubin N Yu *J. Opt. Soc. Am. B* **17** 1509 (2000)